ARTICLE
Journal of Cellular Biochemistry 116:954–968 (2015)

Journal of Cellular Biochemistry

Overexpression of Zinc-Finger Protein 777 (ZNF777) Inhibits Proliferation at Low Cell Density Through Down-Regulation of FAM129A

Ryuzaburo Yuki,[1] Kazumasa Aoyama,[1] Sho Kubota,[1] Noritaka Yamaguchi,[1] Shoichi Kubota,[1] Hitomi Hasegawa,[1] Mariko Morii,[1] Xiayu Huang,[2] Kang Liu,[2] Roy Williams,[2] Michiko N. Fukuda,[2] and Naoto Yamaguchi[1]*

[1]*Department of Molecular Cell Biology, Graduate School of Pharmaceutical Sciences, Chiba University, Chiba 260-8675, Japan*

[2]*Sanford-Burnham Medical Research Institute, La Jolla 92037, California*

ABSTRACT

Krüppel-associated box-containing zinc finger proteins (KRAB-ZFPs) regulate a wide range of cellular processes. KRAB-ZFPs have a KRAB domain, which binds to transcriptional corepressors, and a zinc finger domain, which binds to DNA to activate or repress gene transcription. Here, we characterize ZNF777, a member of KRAB-ZFPs. We show that ZNF777 localizes to the nucleus and inducible overexpression of ZNF777 inhibits cell proliferation in a manner dependent on its zinc finger domain but independent of its KRAB domain. Intriguingly, ZNF777 overexpression drastically inhibits cell proliferation at low cell density but slightly inhibits cell proliferation at high cell density. Furthermore, ZNF777 overexpression decreases the mRNA level of FAM129A irrespective of cell density. Importantly, the protein level of FAM129A strongly decreases at low cell density, but at high cell density the protein level of FAM129A does not decrease to that observed at low cell density. ZNF777-mediated inhibition of cell proliferation is attenuated by overexpression of FAM129A at low cell density. Furthermore, ZNF777-mediated down-regulation of FAM129A induces moderate levels of the cyclin-dependent kinase inhibitor p21. These results suggest that ZNF777 overexpression inhibits cell proliferation at low cell density and that p21 induction by ZNF777-mediated down-regulation of FAM129A plays a role in inhibition of cell proliferation. J. Cell. Biochem. 116: 954–968, 2015.

KEY WORDS: ZNF777; CELL PROLIFERATION; CELL DENSITY; p21; FAM129A; NIBAN

Krüppel-associated box-containing zinc finger proteins (KRAB-ZFPs) consist of approximately one-third of 800 zinc finger proteins and are present only in higher organisms [Bellefroid et al., 1991, 1993; Lupo et al., 2013]. KRAB-ZFPs have been described as potent transcriptional repressors [Margolin et al., 1994; Witzgall et al., 1994; Gebelein and Urrutia, 2001; Lupo et al., 2011]. KRAB-ZFPs consist of a KRAB domain at the N-terminus and a zinc finger domain at the C-terminus, which contains 4 to over 30 zinc fingers [Urrutia, 2003]. The KRAB domain of KRAB-ZFPs binds to transcriptional corepressors, whereas the zinc finger domain of KRAB-ZFPs binds to DNA to activate or repress gene transcription [Friedman et al., 1996; Gebelein et al., 1998; Agata et al., 1999; Looman et al., 2002].

KRAB-ZFPs play important roles in various cellular events, such as cell proliferation, apoptosis, and differentiation. For example, ZNF689 promotes cell proliferation and may play a role in carcinogenesis [Silva et al., 2006]. On the other hand, ZNF23, which is down-regulated in some types of human cancers, inhibits cell proliferation in a manner independent of its KRAB domain [Huang et al., 2007]. However, most of the KRAB-ZFPs are not characterized and their functions are largely unknown.

In this study, we characterized ZNF777, a member of KRAB-ZFPs. We showed that inducible overexpression of ZNF777 inhibits cell proliferation in a manner dependent on its zinc finger domain but independent of its KRAB domain. ZNF777 overexpression drastically

Grant sponsor: Japanese Ministry of Education, Culture, Sports, Science and Technology.
*Correspondence to: Naoto Yamaguchi, Department of Molecular Cell Biology, Graduate School of Pharmaceutical Sciences, Chiba University, Inohana 1–8-1, Chuo-ku, Chiba 260–8675, Japan.
E-mail: nyama@faculty.chiba-u.jp
Manuscript Received: 18 March 2014; Manuscript Accepted: 16 December 2014
Accepted manuscript online in Wiley Online Library (wileyonlinelibrary.com): 5 January 2015
DOI 10.1002/jcb.25046 • © 2015 Wiley Periodicals, Inc.

inhibits cell proliferation at low cell density but slightly inhibits cell proliferation at high cell density. We further showed that ZNF777 overexpression decreased the levels of FAM129A and ZNF777-mediated down-regulation of FAM129A induces moderate levels of the cyclin-dependent kinase inhibitor p21 at low cell density, resulting in a delay in the G2/M phase.

MATERIALS AND METHODS

PLASMIDS

ZNF777(1st ATG) and ZNF777(2nd ATG) were constructed from cDNA corresponding to the nucleotide sequence 65–2659 and 181–2659 of human ZNF777 (ZNF777) (NM_015694.2), respectively. These constructs were subcloned into the pcDNA4/TO vector, as described previously [Kasahara et al., 2007]. To construct ZNF777-wt, the FLAG epitope was linked to ZNF777(1st ATG) at the N-terminus. The sequence A-A-I-D was inserted between the FLAG epitope and ZNF777(1st ATG), and this construct was subcloned into the pcDNA4/TOneo vector (pcDNA4/TOneo/ZNF777-wt), which was generated as described [Nakayama et al., 2009]. ZNF777-Δzinc was constructed from pcDNA4/TOneo/ZNF777-wt by SacII and BsrGI digestion, blunting, and ligation, resulting in the insertion sequence T-K-L-A-L before the stop codon. ZNF777-ΔKRAB was generated as follows. The DNA fragment corresponding to the amino acid sequence 1–247 of ZNF777(1st ATG) was amplified by PCR using the sense primer 5′-TCCACGCTGTTTTTGACCTCC-3′ and the antisense primer 5′-ATGACTCCGCGGTTCAGATGGTTCGCGAACTCC-3′. The EcoRI-SacII fragment of the PCR product was subcloned into pcDNA4/TOneo/ZNF777-wt. To construct NLS-ZNF777-Δzinc, ZNF777-Δzinc was linked to the FLAG epitope, the HA epitope, and a nuclear localization signal (NLS) at the N-terminus, as described previously [Aoyama et al., 2011]. The sequence L-D-G-G-Y-P was inserted between the FLAG epitope and the HA epitope. The sequence G-G-L was inserted between the HA epitope and the NLS. The sequence V-L-D-P-A-Q-W-R-P-R-I-D was inserted between the NLS and ZNF777-Δzinc. For expression in mammalian cells, this construct was subcloned into the pcDNA4/TOneo vector. cDNA encoding human FAM129A (Niban; Open Biosystems) was subcloned into the pEBMulti-Puro vector (pEBMulti-Puro/FAM129A) (Wako Pure Chemical Industries, Osaka).

RNA INTERFERENCE

Knockdown of ZNF777 and FAM129A was performed with short hairpin RNA (shRNA) for silencing ZNF777 (#1, GGCTCA-GAAAGTTTGGAGA; #2, GCTCTACAAGAACGTGATG) and FAM129A (#1, AGAGATTTAACGTCACAGTTT; #2, GTGGAAG-GAGAGATACGTT), respectively. The nucleotides for shRNA were annealed and subcloned into the BglII-XbaI site of the EGFP-pENTR4/H1 or the pENTR4/H1 vector (provided by H. Miyoshi) [Obata et al., 2010]. To establish a ZNF777-stable knockdown cell line, HeLa S3 cells were co-transfected with pENTR4/H1/ZNF777-shRNA#1 and a plasmid containing the hygromycin resistant gene, and selected in 250 μg/ml hygromycin. pEBMulti-Neo/ZNF777-shRNA and pEBMulti-Neo/FAM129A-shRNA were generated as follows. The DNA fragment corresponding to the H1 promoter and ZNF777-shRNA or FAM129A-shRNA was amplified by PCR using the sense primer 5′-GTTGTCGACGGTACCAC-TAGTCATCAACCCGCTCCAAGGAATCGC-3′ and the antisense primer 5′-TATACTAGTCGACGGTACCTGTTCGTTGCAACAAATT-GATAAGCAATGCT-3′. The SpeI-SpeI fragment of the PCR product was subcloned into the pEBMulti-Neo vector (Wako Pure Chemical Industries, Osaka). To establish ZNF777 or FAM129A knockdown cells, HeLa S3 cells were transfected with pEBMulti-Neo/ZNF777-shRNA or pEBMulti-Neo/FAM129A-shRNA, and selected in 520 μg/ml G418 for 5 days.

ANTIBODIES

The following antibodies were used: ZNF777 (ZNF777, NBP1–03344; Novus Biologicals), FLAG (M2 and polyclonal antibody; Sigma), FAM129A (Niban; Signalway Antibody), actin (clone C4; CHEMICON International), hsc70 (B-6; Santa Cruz Biotechnology), normal rabbit IgG (Santa Cruz Biotechnology), lamin A/C (N-18; Santa Cruz Biotechnology), $cPLA_2$ (Santa Cruz Biotechnology), Ku70 (C-19; Santa Cruz Biotechnology), p21 (12D1; Cell Signaling Technology), Phospho-p44/42 MAP kinase Thr^{202}/Tyr^{204} (pERK1/2, E10; New England BioLabs), ERK2 (C-14; Santa Cruz Biotechnology), and α-tubulin (Serotec). Horseradish peroxidase (HRP)-$F(ab')_2$ secondary antibodies were purchased from Amersham Biosciences. FITC-IgG, and Alexa Fluor 488- and Alexa Fluor 647-labeled IgG secondary antibodies were purchased from BioSource International and Invitrogen.

CELLS AND TRANSFECTION

HeLa S3, HeLa (Japanese Collection of Research Bioresources, Osaka), and HCT116 cells were cultured in Iscove's modified DME supplemented with 1% fetal bovine serum (FBS) and 4% bovine serum (BS). Cells seeded in a 35 mm culture dish were transiently transfected with 1 μg of plasmid DNA using 5 μg of linear polyethylenimine (25 kDa) (Polyscience, Inc.) [Fukumoto et al., 2010]. HeLa S3 cell clones expressing ZNF777-wt, ZNF777-Δzinc, NLS-ZNF777-Δzinc, or ZNF777-ΔKRAB were generated in an inducible manner [Kasahara et al., 2007]. HeLa S3/TR (clone A3f5) cells, which stably express the tetracycline repressor (TR) [Kuga et al., 2008; Aoyama et al., 2011], were transfected with pcDNA4/TOneo/ZNF777-wt, pcDNA4/TOneo/ZNF777-Δzinc, pcDNA4/TOneo/ZNF777-ΔKRAB, or pcDNA4/TOneo/NLS-ZNF777-Δzinc, and cell clones expressing inducible ZNF777-wt (HeLa S3/ZNF777-wt), ZNF777-Δzinc (HeLa S3/ZNF777-Δzinc), ZNF777-ΔKRAB (HeLa S3/ZNF777-ΔKRAB), or NLS-ZNF777-Δzinc (HeLa S3/NLS-ZNF777-Δzinc) were selected in 600 μg/ml G418. A HCT116 cell clone expressing inducible ZNF777-wt (HCT116/TR/ZNF777-wt) was generated from HCT116/TR (clone 0.8G5) cells [Soeda et al., 2013] transfected with pcDNA4/TOneo/ZNF777-wt. To induce ZNF777-wt, ZNF777-Δzinc, NLS-ZNF777-Δzinc or ZNF777-ΔKRAB, doxycycline (Dox), an analog of tetracycline, was used at 1000 ng/ml, unless otherwise stated. To stably overexpress FAM129A in cells expressing inducible ZNF777-wt, cell clones expressing inducible ZNF777-wt were transfected with pEB-Multi-Puro/FAM129A, and selected in 350 ng/ml puromycin for 5 days.

CELL PROLIFERATION AND VIABILITY ASSAY

Cells seeded at $0.5\sim20\times10^4$ cells in a 35 mm culture dish ($500\sim20{,}000$ cells/cm^2) were treated with (+) or without (−) Dox after 1 day of culture and subsequently cultured for 4 or 8 days with medium change every other day. Cells were trypsinized on 1, 3, 4, 6, and 8 days of culture, and viable and dead cell numbers were counted using trypan blue.

WESTERN BLOTTING

Cells were seeded at $500\sim20{,}000$ cells/cm^2 in a 35 mm (or 60 mm) culture dish. Cell lysates were prepared in SDS-PAGE sample buffer and subjected to SDS-PAGE and electrotransferred onto polyvinylidene difluoride membranes (Millipore). Immunodetection was performed by enhanced chemiluminescence (Millipore), as described [Ishibashi et al., 2013; Kubota et al., 2013, 2014]. Results were analyzed using a ChemiDoc XRS-Plus image analyzer (Bio-Rad). Intensity of chemiluminescence was measured using Quantity One software (Bio-Rad). Composite figures were prepared using GNU Image Manipulation Program version 2.6.11 software (GIMP) and Illustrator 16.0.4 software (Adobe).

IMMUNOFLUORESCENCE

Confocal and differential-interference-contrast (DIC) images were obtained using a Fluoview FV500 confocal laser scanning microscope with a 40×1.00 NA objective (Olympus, Tokyo) and an LSM 510 confocal laser scanning microscope with a 63×1.40 NA oil immersion objective (Zeiss), as described recently [Aoyama et al., 2013; Soeda et al., 2013]. One planar (xy) section slice (1.0- or 2.0 μm thickness) was shown in all experiments. In brief, cells were fixed in 4% paraformaldehyde for 20 min at room temperature or 100% methanol for 1 min at −20°C, and permeabilized in phosphate-buffered saline (PBS) containing 0.1% saponin and 3% bovine serum albumin at room temperature [Aoyama et al., 2011]. Cells were subsequently reacted with appropriate primary antibodies for 1 h, washed with PBS containing 0.1% saponin, and stained with FITC-, Alexa Fluor 488- or Alexa Fluor 647-conjugated secondary antibodies for 1 h. For DNA staining, cells were treated with 200 μg/ml RNase A and 20 μg/ml propidium iodide (PI) for 30 min, and mounted in *p*-phenylenediamine-PBS-glycerol. For staining of endogenous ZNF777, HCT116 cells were prefixed with 0.4% paraformaldehyde for 5 min at room temperature, extracted with 0.1% Triton X-100 for 3 min on ice, and fixed with 4% paraformaldehyde for 20 min at room temperature. Composite figures were prepared using GIMP 2.6.11 and Illustrator 16.0.4.

FLOW CYTOMETRY

For cell-cycle analysis, cells detached by trypsinization were fixed in 4% paraformaldehyde for 1 h, and permeabilized with 70% ethanol for at least 1 h at −30°C [Kubota et al., 2014]. Fixed cells were permeabilized and blocked in PBS containing 0.1% saponin and 3% bovine serum albumin (BSA) for 30 min at room temperature. After washing with PBS containing 0.1% Tween 20, cells were reacted with anti-FLAG antibody for 1 h at room temperature, then stained with AF647-conjugated anti-rabbit IgG antibody for 1 h. Subsequently, cells were treated with 200 μg/ml RNase A and 50 μg/ml PI at 37 °C for 30 min to stain DNA. A minimum of 6,000 cells per sample was analyzed by flow cytometry using a Guava easyCyte (Millipore) equipped with a 488 nm blue laser and a 640 nm red laser using liner amplification. Data were analyzed using Flowing Software version 2.5.1 (Perttu Terho, Centre for Biotechnology, Turku, Finland). Cell debris was excluded by gating on forward scatter and pulse-width profiles.

SUBCELLULAR FRACTIONATION

Subcellular fractionation was performed as described recently [Kubota et al., 2013]. In brief, cell pellets were washed with PBS and resuspended in Low-salt buffer (10 mM HEPES, pH 7.4, 10 mM KCl, 0.1% Triton X-100, 0.34 M sucrose, 10% glycerol, 1.7 mM $MgCl_2$, 10 mM NaF, 4 mM β-glycerophosphate, 2 mM Na_3VO_4, 50 μg/ml aprotinin, 100 μM leupeptin, 25 μM pepstatin A, and 2 mM PMSF), and the cells were kept on ice for 10 min. Cytosolic proteins were separated from nuclei by centrifugation at 2,000 g for 5 min. Isolated nuclei were lysed in High-salt buffer (50 mM HEPES, pH 7.4, 300 mM KCl, 1.0% Triton X-100, 20% glycerol, 50 mM NaF, 10 mM β-glycerophosphate, 10 mM Na_3VO_4, 1 mM EDTA, 50 μg/ml aprotinin, 100 μM leupeptin, 25 μM pepstatin A, and 2 mM PMSF). After 20 min incubation on ice, soluble nuclear proteins were separated from chromatin by centrifugation at 17,900 *g* for 10 min. The resulting chromatin fraction was once washed with High-salt buffer, solubilized in SDS sample buffer and sheared by sonication.

SENESCENCE-ASSOCIATED (SA) β-GALACTOSIDASE ACTIVITY

SA-β-gal activity was detected as described previously [Kikuchi et al., 2010]. In brief, cells were fixed in 0.2% glutaraldehyde plus 1.85% formaldehyde in PBS at room temperature for 5 min. Fixed cells were washed with PBS and then incubated with 1 mg/ml X-gal (5-bromo-4-chloro-3-indolyl-β- D-galactopyranoside) at 37 °C for 14 h in staining solution (40 mM sodium citrate-phosphate, pH 6.0, 4 mM potassium ferrocyanide, 4 mM potassium ferricyanide, 150 mM NaCl, and 2 mM $MgCl_2$).

SEMIQUANTITATIVE RT-PCR

Cells were seeded at $500\sim20{,}000$ cells/cm^2 in a 35 mm (or 60 mm) culture dish. Total RNAs were isolated from cells with the ISOGEN reagent (Nippon Gene, Tokyo) or the TRIzol reagent (Invitrogen), and cDNAs were synthesized from 0.5 or 1 μg of each RNA preparation using the PrimeScript RT reagent Kit (TakaraBio, Shiga), as described [Ishibashi et al., 2013]. Genes of which expression levels were changed by ZNF777-wt expression were identified as described [Chernov et al., 2010]. To avoid saturation of PCR products, conditions of PCR were optimized before semiquantitative RT-PCR was carried out. The primers used for PCR are as follows: FAM129A, 5′-AATCACACTTCCCACTGTGC-3′ (sense) and 5′-GTTTCTTCAAGATAGCAGCTTCC-3′ (antisense); ZNF777, 5′-CGGGATATCGACATGGAGAACAACGCTC-3′ (sense) and 5′-ATGACTCCGCGGTTCAGATGGTTCGCGAACTCC-3′ (antisense); glyceraldehyde 3-phosphate dehydrogenase (GAPDH), 5′-ACCACAGTCCATGCCATCAC-3′ (sense) and 5′-TCCACCACCCTGTTGCTGTA-3′ (antisense) [Aoyama et al., 2011; Ishibashi et al., 2013]. The sizes of PCR products are 192 bp for FAM129A, 728 bp for ZNF777-wt and ZNF777-Δzinc, and 452 bp for GAPDH. Amplification was carried out using a T100 Thermal Cycler (BioRad) or an MJ mini thermal cycler (BioRad) with Ex Taq

DNA polymerase (TakaraBio) under the following conditions: For FAM129A, initial heating at 94 °C for 2 min, followed by 27 cycles of denaturation at 94 °C for 30 s, annealing at 53 °C for 30 s and extension at 72 °C for 1 min. For ZNF777-wt and ZNF777-Δzinc, initial heating at 95 °C for 2 min, followed by 20 cycles of denaturation at 95 °C for 30 s, annealing at 54 °C for 30 s and extension at 72 °C for 90 s. For GAPDH, initial heating at 94 °C for 2 min, followed by 25 cycles of denaturation at 94 °C for 30 sec, annealing at 56 °C for 30 s and extension at 72 °C for 1 min. The products of RT-PCR were electrophoresed on a 2% agarose gel containing ethidium bromide. The density of each amplified fragment was quantitated using a ChemiDoc XRSPlus image analyzer and Quantity One software.

RESULTS

DETERMINATION OF THE TRANSLATION INITIATION SITE OF ZNF777

First, we noticed two ATG codons in the 5′ mRNA region of ZNF777 in accordance with the Kozak consensus sequence (Fig. 1A, lower panels). To determine the actual translation initiation site of ZNF777, we constructed two expression vectors encoding ZNF777 cDNAs initiating from the 1st ATG [ZNF777(1st ATG)] and the 2nd ATG [ZNF777(2nd ATG)] (Fig. 1A, upper panels). ZNF777(1st ATG) and ZNF777(2nd ATG) had apparent molecular masses of 130 and 124 kDa (Fig. 1B), respectively, and these were approximately 35 kDa higher than the predicted molecular masses. This retardation of electrophoretic mobility might be explained by some post-translational modification. Then, to detect endogenous ZNF777, sufficient amounts of lysates from cells transfected with vector were loaded on an SDS-PAGE gel. A band corresponding to ZNF777(1st ATG) at 130 kDa was detected (Fig. 1C) and shRNA against ZNF777 [ZNF777-shRNA#1] specifically decreased the intensity of the 130 kDa band (Fig. 1D). These results suggest that endogenous ZNF777 is translated from the 1st ATG.

NUCLEAR LOCALIZATION OF ENDOGENOUS ZNF777

To examine the subcellular localization of endogenous ZNF777, HCT116 cells were stained with control or anti-ZNF777 antibody. When cells were prefixed with 0.4% paraformaldehyde and extracted with 0.1% Triton X-100 before fixation with 4% paraformaldehyde, endogenous ZNF777 was clearly detected in the nucleus (Fig. 2A). Triton X-100 extraction before fixation could permit anti-ZNF777 antibody to access the epitope on nuclear ZNF777 possibly by extracting adjacent proteins. Treatment with ZNF777 shRNA [ZNF777-shRNA#1] decreased the anti-ZNF777 immunofluorescence intensity in the nucleus (Fig. 2B). To substantiate the nuclear localization of endogenous ZNF777, cells were subfractionated into the Low-salt soluble, the High-salt soluble, and the High-salt insoluble fractions (see MATERIALS AND METHODS). As described recently [Kubota et al., 2013], the Low-salt soluble fraction contained the cytosolic protein cPLA2, and the High-salt soluble fraction contained the chromatin-binding protein Ku70. The High-salt insoluble fraction contained the nuclear matrix protein lamin A/C. We found that endogenous ZNF777 was predominantly present in the High-salt soluble fraction but not in the Low-salt soluble and the High-salt insoluble fractions (Fig. 2C). These results support that endogenous ZNF777 is mainly localized to the nucleus as a chromatin-binding protein.

INHIBITION OF CELL PROLIFERATION BY ZNF777 EXPRESSION

We constructed FLAG-tagged ZNF777(1st ATG) (ZNF777-wt) and established stable HeLa S3 cell lines expressing inducible ZNF777-wt. Western blot analysis showed that treatment with 1000 ng/ml doxycycline (Dox) induced the overexpression of ZNF777-wt (Fig. 3A). When cells were extracted with Triton X-100 before fixation, overexpressed ZNF777-wt was detected in the nucleus similar to endogenous ZNF777 (Fig. 3B; see also Fig. 2A). To examine the effect of ZNF777 overexpression on cell proliferation, parental HeLa S3/TR cells and HeLa S3/TR cells expressing inducible ZNF777-wt were seeded at a cell density of 500 cells/cm^2, treated with or without 1000 ng/ml Dox after 1 day of culture, and subsequently cultured for a further 7 days. Dox treatment decreased viable cell numbers in cells expressing inducible ZNF777-wt but not in parental cells (Fig. 3C). The number of dead cells was increased in cells expressing inducible ZNF777-wt upon Dox treatment. Without Dox treatment [Dox(−)], viable cell numbers of cells expressing inducible ZNF777-wt were decreased compared with those of parental cells (Fig. 3C, compare inducible expression:ZNF777-wt with inducible expression:none), because the expression of ZNF777-wt [Dox(−)] was unexpectedly observed and the leaking expression level was approximately two- to four-fold higher than that of endogenous ZNF777 (Fig. 3A). We examined whether cell proliferation could be affected by mild expression of ZNF777. Western blot analysis showed that ZNF777-wt expression was induced in a Dox concentration-dependent manner (Fig. 3D). The leaking expression of ZNF777 was visible at 0 ng/ml Dox (Fig. 3D, longer exposure; see also Fig. 3A). Inhibition of cell proliferation was evident upon treatment with 0.01∼0.06 ng/ml Dox, and treatment with 0.1, 1, and 1000 ng/ml Dox strongly inhibited cell proliferation (Fig. 3E). Moreover, knockdown of endogenous ZNF777 by two different shRNAs did not affect cell proliferation in HeLa S3 cells (Fig. 3F, 3G), suggesting the possibility that the expression levels of endogenous ZNF777 are insufficient to affect HeLa cell proliferation. Taken together, these results suggest that overexpression of ZNF777 is involved in inhibition of HeLa cell proliferation.

Next, we examined whether a cyclin-dependent kinase inhibitor was involved in ZNF777 expression-mediated cell proliferation inhibition. We found that p21 expression was induced upon ZNF777-wt expression in a Dox concentration-dependent manner (Fig. 3H, 3I). The expression level of p21 in cells expressing ZNF777-wt treated with 1000 ng/ml Dox was approximately three times as high as that in parental cells without Dox treatment, although the ZNF777-induced expression levels of p21 were much lower than that seen in cell-cycle arrested cells treated with Adriamycin (ADR) (Fig. 3I). To examine the effect of ZNF777 overexpression on the cell cycle, we synchronized cells expressing inducible ZNF777-wt using a double-thymidine block and analyzed DNA contents by flow cytometry. Cells that were synchronized in the G1/S phase appeared to progress normally into the G2/M phase 12 h after release from double-thymidine block. However, 18 h after release from double-thymidine block, the number of G2/M-phase cells was increased and

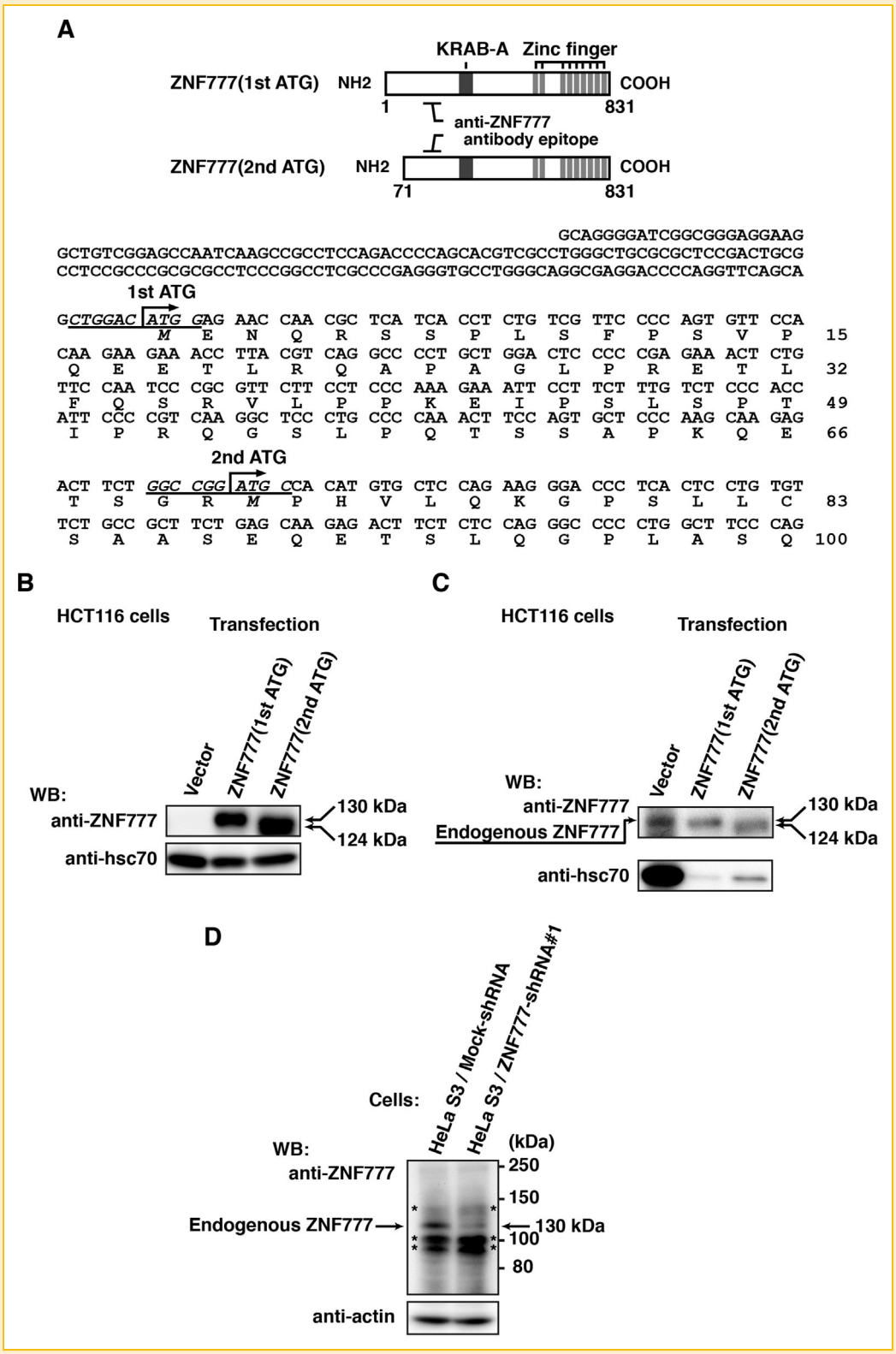

Fig. 1. Determination of the translation initiation site of ZNF777. (A) (Upper) Schematic representations of ZNF777. KRAB, Krüppel-associated box. (Lower) The nucleotide and deduced amino acid sequence of the 5′end of ZNF777 mRNA. The Kozak sequences and the translation initiation methionines are shown underlined and italicized. The numbers on the right indicate the amino acid number from the 1st translation initiation methionine. (B, C) HCT116 cells transfected with vector alone, ZNF777(1st ATG), or ZNF777(2nd ATG) were cultured for 24 h. Whole cell lysates were subjected to Western blotting, using anti-ZNF777 and anti-hsc70 antibodies. Full-length blots are presented in Supplementary Fig. S1A and S1B. (D) Whole cell lysates from HeLa S3/Mock-shRNA or HeLa S3/ZNF777-shRNA#1 cells were subjected to Western blotting, using anti-ZNF777 and anti-actin antibodies. Asterisks show nonspecific bands. Full-length blots are presented in Supplementary Fig. S1C.

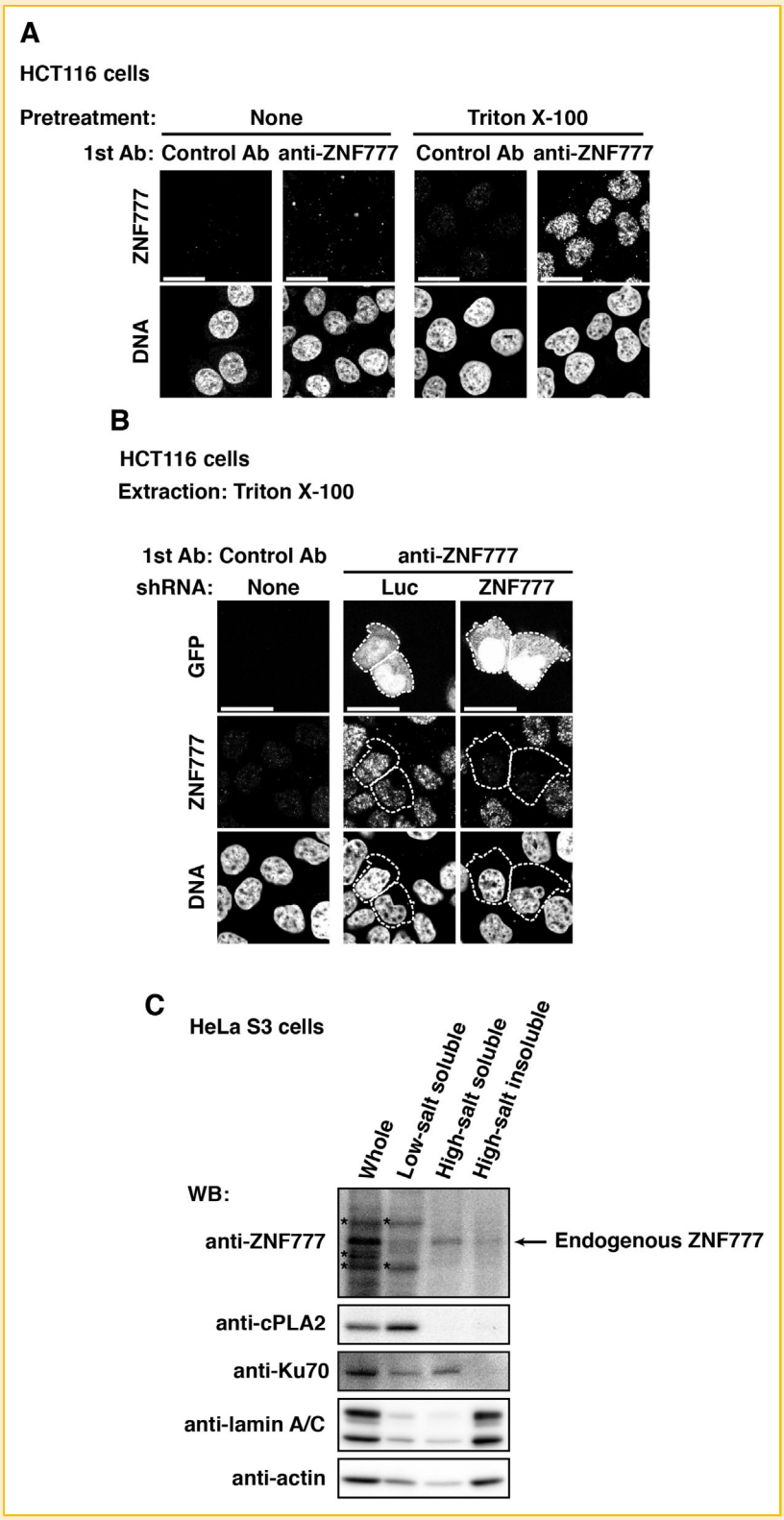

Fig. 2. Nuclear localization of endogenous ZNF777. (A) HCT116 cells pretreated with 0.4% paraformaldehyde plus Triton X-100 or not were fixed with 4% paraformaldehyde and doubly stained with control or anti-ZNF777 antibody and propidium iodide (PI). Scale bars, 20 μm. (B) HCT116 cells transfected with shRNA against luciferase (Luc) or ZNF777 [ZNF777-shRNA#1] were cultured for 48 h. Cells were extracted and fixed with paraformaldehyde with or without Triton X-100, and doubly stained with control or anti-ZNF777 antibody and PI. Broken lines indicate the outlines of GFP-positive cells that are transfected with shRNA against luc or ZNF777. Scale bars, 20 μm. (C) HeLa S3 cells were subjected to chromatin fractionation as described under 'MATERIALS AND METHODS'. Immunoblotting was performed for ZNF777, $cPLA_2$, Ku70, lamin A/C, and actin. Asterisks show nonspecific bands. Full-length blots are presented in Supplementary Fig. S2.

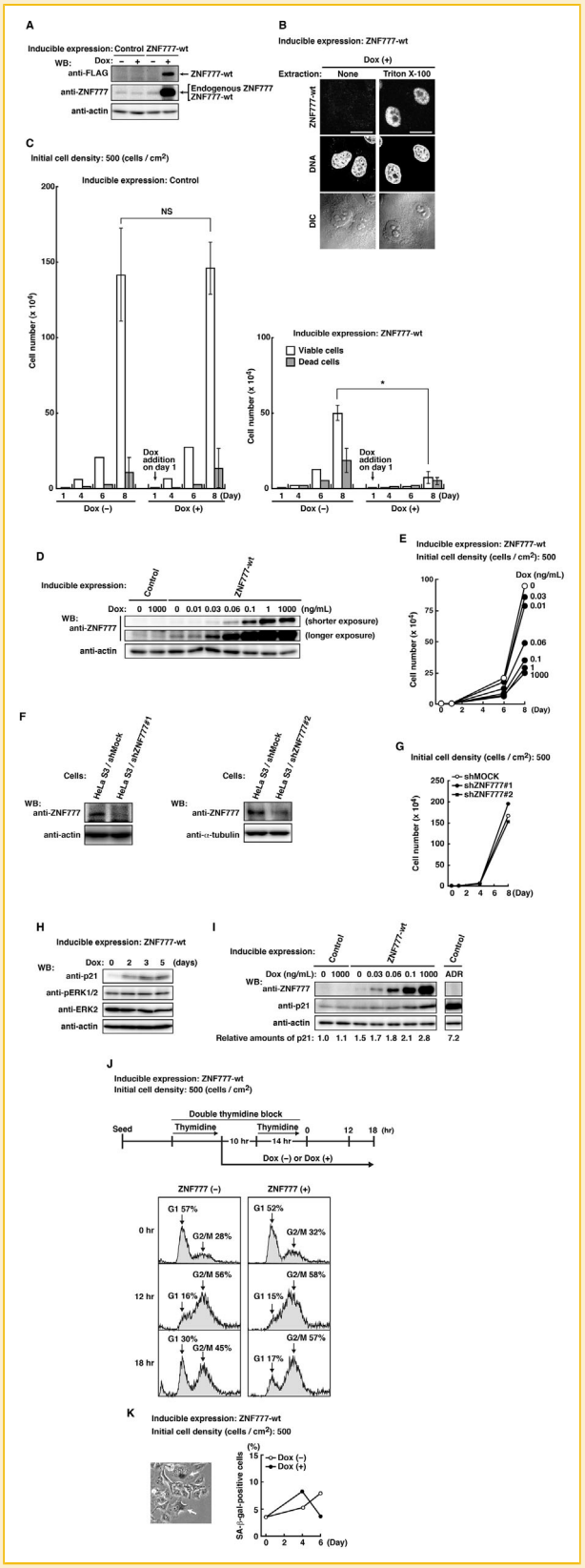

Fig. 3. Continued.

the number of G1-phase cells was decreased upon ZNF777-wt expression (Fig. 3J), suggesting that a delay in the G2/M phase is caused possibly through moderate levels of p21 induction. Moreover, ZNF777-wt expression did not induce SA-β-gal activity-positive senescent cells (Fig. 3K). Taken together, these results suggest that a delay in the G2/M phase is involved in ZNF777 expression-mediated inhibition of cell proliferation.

ZNF777-MEDIATED INHIBITION OF CELL PROLIFERATION DEPENDENT ON CELL DENSITY

To examine the role of cell density in ZNF777-mediated inhibition of cell proliferation, cells expressing inducible ZNF777-wt seeded at cell densities of 500, 2,000, or 20,000 cells/cm^2 were treated with or without Dox after 1 day of culture and subsequently cultured for

Fig. 3. Inhibition of cell proliferation by ZNF777. (A) Parental HeLa S3/TR cells and HeLa S3 cells expressing inducible ZNF777-wt were treated with (+) or without (–) doxycycline (Dox) for 1 day. Whole cell lysates were subjected to Western blotting, using anti-FLAG, anti-ZNF777, and anti-actin antibodies. Full-length blots are presented in Supplementary Fig. S3A. (B) Cells expressing inducible ZNF777-wt were cultured with Dox for 1 day. Cells were treated with or without Triton X-100, fixed with paraformaldehyde, and doubly stained with anti-FLAG antibody and PI. DIC, differential interference-contrast. Scale bars, 20 μm. (C) Parental cells and cells expressing inducible ZNF777-wt were seeded at 500 cells/cm^2, treated with (+) or without (–) Dox after 1 day of culture, and subsequently cultured for 7 days. Cell numbers were counted. Viable and dead cell numbers were plotted. Bars represent means ± S.D. from three independent experiments. An asterisk indicates the significant difference ($^*P < 0.05$; NS, not significant) calculated by Student's *t*-test. (D) Parental cells and cells expressing inducible ZNF777-wt were seeded and treated with Dox at the indicated concentrations for 2 days. Whole cell lysates were subjected to Western blotting, using anti-ZNF777 and anti-actin antibodies. Full-length blots are presented in Supplementary Fig. S3B. (E) Cells expressing inducible ZNF777-wt were seeded at 500 cells/cm^2, treated with Dox at the indicated concentrations after 1 day of culture, and subsequently cultured for 7 days. Cell numbers were counted, and viable cell numbers were plotted. (F) Whole cell lysates from HeLa S3/Mock-shRNA, HeLa S3/ZNF777-shRNA#1, or HeLa S3/ZNF777-shRNA#2 cells were subjected to Western blotting, using anti-ZNF777 and anti-actin or anti-α-tubulin antibodies. Full-length blots are presented in Supplementary Fig. S4A. (G) HeLa S3/Mock-shRNA, HeLa S3/ZNF777-shRNA#1, or HeLa S3/ZNF777-shRNA#2 cells seeded at 500 cells/cm^2 were cultured for 7 days. Cell numbers were counted, and viable cell numbers were plotted. (H) Cells expressing inducible ZNF777-wt were treated Dox for 0∼5 days. Whole cell lysates were subjected to Western blotting, using anti-p21, anti-pERK1/2, anti-ERK2, and anti-actin antibodies. Full-length blots are presented in Supplementary Fig. S4B. (I) Parental cells and cells expressing inducible ZNF777-wt were seeded and treated with Dox or 30 ng/ml Adriamycin (ADR) at the indicated concentrations for 3 days. Whole cell lysates were subjected to Western blotting, using anti-ZNF777, anti-p21, and anti-actin antibodies. Full-length blots are presented in Supplementary Fig. S5. (J) Schematic depiction of our synchronization method. Cells expressing inducible ZNF777-wt were seeded at 500 cells/cm^2, synchronized using a double thymidine block, and subsequently released into thymidine-free medium for 12∼18 h. Cells were stained with anti-FLAG antibody and PI for analyzing cell cycle progression by flow cytometry. Histograms of ZNF777-wt-expressing cells with Dox treatment [ZNF777(+)] and non-expressing cells without Dox treatment [ZNF777(–)] in cells expressing inducible ZNF777-wt were shown. (K) Cells expressing inducible ZNF777-wt were seeded at 500 cells/cm^2, and treated with (+) or without (–) Dox for 1∼5 days. Cells were fixed and examined for SA-β-galactosidase activity. Cells cultured for 5 days without Dox were shown by phase-contrast microscopy (left). Arrows indicate SA-β-gal-positive cells. The number of SA-β-gal-positive cell was plotted (right).

7 days. 92% and 72% reductions in cell proliferation were observed upon ZNF777-wt induction at 500 cells/cm^2 (low cell density) and 2,000 cells/cm^2 (intermediate cell density) (Fig. 4A), respectively. However, at 20,000 cells/cm^2 (high cell density), overexpression of ZNF777-wt showed a 29% reduction in cell proliferation (Fig. 4A). The ratios of the number of dead cells to the number of viable cells were decreased at high cell density upon ZNF777-wt induction (Fig. 4B, Dox(+)). Upon ZNF777-wt induction at low cell density, the number of viable cells increased in a manner dependent on increasing concentrations of conditioned medium derived from cells at high cell density (Fig. 4C), which may be explained by the possibility that conditioned medium derived from high-density cells is rich in a secreted putative growth factor(s). Furthermore, we examined whether ZNF777 inhibited cell proliferation in HCT 116 cells in a cell density-dependent manner. We established stable HCT116 cell lines expressing inducible ZNF777-wt, and Western blot analysis showed that Dox treatment induced overexpression of ZNF777-wt (Fig. 4D). Similar to HeLa S3 cells, HCT116 cells exhibited inhibition of cell proliferation at low cell density upon ZNF777-wt expression (Fig. 4E). These results suggest that overexpression of ZNF777-wt inhibits cell proliferation in particular at low cell density.

ROLE OF THE ZINC FINGER DOMAIN IN INHIBITION OF CELL PROLIFERATION

We constructed two ZNF777-wt mutants lacking the zinc finger domain (ZNF777-Δzinc) and the KRAB domain (ZNF777-ΔKRAB) (Fig. 5A) and established stable cell lines expressing inducible ZNF777-Δzinc or ZNF777-ΔKRAB. Western blot analysis showed that Dox treatment induced the expression of ZNF777-Δzinc or ZNF777-ΔKRAB as well as that of ZNF777-wt (Fig. 5B). ZNF777-Δzinc had the apparent molecular mass of 95 kDa, which was approximately 35 kDa higher than the predicted molecular mass. On the other hand, ZNF777-ΔKRAB had the apparent molecular mass of 67 kDa close to the predicted molecular mass. These results suggest that the KRAB domain of ZNF777 is responsible for electrophoretic mobility retardation of ZNF777.

To examine the role of the zinc finger domain and the KRAB domain in nuclear localization of ZNF777, cells expressing inducible ZNF777-wt, ZNF777-Δzinc, or ZNF777-ΔKRAB were treated with or without Dox and fixed with methanol. Intriguingly, ZNF777-Δzinc was seen in the cytoplasm, whereas ZNF777-ΔKRAB was seen in the nucleus (Fig. 5C). These results suggest that the zinc finger domain but not the KRAB domain is involved in the nuclear localization of ZNF777.

Next, to examine the role of the zinc finger domain and the KRAB domain in ZNF777-mediated inhibition of cell proliferation, cells expressing inducible ZNF777-wt, ZNF777-Δzinc, or ZNF777-ΔKRAB at a cell density of 500 cells/cm^2 were treated with or without Dox after 1 day of culture and subsequently cultured for 7 days. The expression of ZNF777-Δzinc was incapable of inhibiting cell proliferation, whereas ZNF777-ΔKRAB expression obviously inhibited cell proliferation as well as ZNF777-wt (Fig. 5D). Moreover, to substantiate the nuclear role of the zinc finger domain in ZNF777-mediated inhibition of cell proliferation, we constructed NLS-ZNF777-Δzinc by linking a nuclear localization signal (NLS) to ZNF777-Δzinc. To compare the localization of NLS-ZNF777-Δzinc with that of ZNF777-wt and ZNF777-Δzinc, cells transfected with NLS-ZNF777-Δzinc, ZNF777-Δzinc or ZNF777-wt were triply stained with anti-FLAG and anti-ZNF777 antibodies and PI for DNA. Unlike ZNF777-Δzinc, NLS-ZNF777-Δzinc was observed in the nucleus as well as ZNF777-wt (Fig. 5E). We established stable cell lines expressing inducible NLS-ZNF777-Δzinc. Western blot analysis showed that Dox treatment induced the expression of NLS-ZNF777-Δzinc (Fig. 5F). Despite its nuclear localization, the expression of NLS-ZNF777-Δzinc hardly inhibited cell proliferation (Fig. 5G). Taken together, these results suggest that the zinc finger domain of ZNF777 plays a critical role in inhibition of cell proliferation.

INVOLVEMENT OF DOWN-REGULATION OF FAM129A IN ZNF777-MEDIATED INHIBITION OF CELL PROLIFERATION

We searched for genes of which expression levels were changed upon ZNF777-wt induction and found that the expression of ZNF777-wt decreased mRNA levels of FAM129A (Fig. 6A), whose activity is involved in protein translation [Sun et al., 2007]. Western blot analysis confirmed that ZNF777-wt overexpression decreased protein levels of FAM129A (Fig. 6B). The protein levels of FAM129A were decreased in a Dox concentration-dependent manner, and the protein level of ZNF777 inversely correlated with that of FAM129A (Fig. 6C). The protein levels of FAM129A were decreased in cells expressing inducible-wt without Dox treatment compared with parental cells (Fig. 6C), because the leaking expression of ZNF777-wt was again seen in cells expressing ZNF777-wt. In addition, ZNF777-wt expression decreased mRNA levels of FAM129A both at 500 and 20,000 cells/cm^2 (Fig. 6D). However, the expression of ZNF777-Δzinc did not affect the mRNA and protein levels of FAM129A (Fig. 6E, 6F). Furthermore, a ZNF777-mediated decrease in the protein level of FAM129A was also observed in HCT116 cells expressing inducible ZNF777-wt (Fig. 6G).

To examine whether a decrease in mRNA levels of FAM129A was involved in ZNF777-mediated inhibition of cell proliferation, we overexpressed FAM129A in cells expressing inducible ZNF777-wt. Overexpression of FAM129A was detected upon the induction of ZNF777-wt (Fig. 6H). Although 55% reduction in cell proliferation was observed upon ZNF777-wt induction, ZNF777-wt induction together with FAM129A overexpression exhibited only 33% reduction in cell proliferation (Fig. 6I). Because FAM129A overexpression did not completely rescue ZNF777-mediated inhibition of cell proliferation, we hypothesized that ZNF777-regulated genes other than FAM129A may be also involved in inhibition of cell proliferation. Taken together, these results suggest that a decrease in the level of FAM129A partly contributes to ZNF777-mediated inhibition of cell proliferation.

A LINK BETWEEN A DECREASED LEVEL OF FAM129A AND AN INHIBITION RATE OF CELL PROLIFERATION

Methanol fixation, which is suitable for immunostaining of both cytosolic and nuclear proteins, showed that the nuclear localization of ZNF777-wt was not affected by cell density (Fig. 7A). High cell density rather increased the induction levels of ZNF777-wt than low cell density (Fig. 7B). To examine the effect of cell density on the

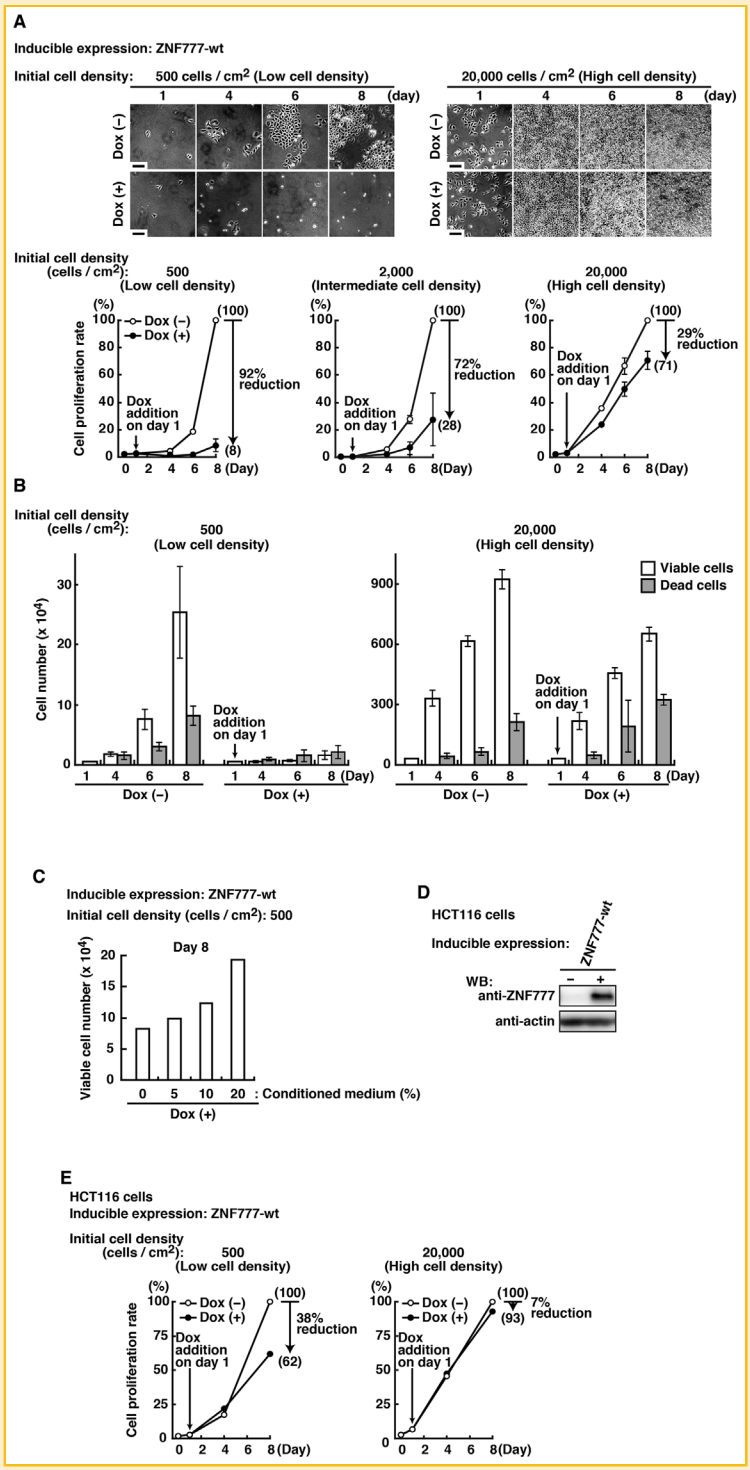

Fig. 4. Cell density-dependent, ZNF777-mediated inhibition of cell proliferation. (A, B) HeLa S3 cells expressing inducible ZNF777-wt were seeded at 500, 2,000, or 20,000 cells/cm^2, treated with (+) or without (−) Dox after 1 day of culture, and subsequently cultured for 7 days. Cells cultured for 1, 4, 6, and 8 days were shown by phase-contrast microscopy (A, upper). Cell numbers were counted, and cell proliferation rates were assessed by measuring the percent ratio of the viable cell number on each day to that on day 8 in the absence of Dox (A, lower). Viable and dead cell numbers were plotted (B). Bars represent means ± S.D. from three independent experiments. Numbers in parentheses indicate mean values. (C) HeLa S3 cells expressing inducible ZNF777-wt were seeded at 500 cells/cm^2, treated with Dox plus 0–20% conditioned medium after 1 day of culture, and subsequently cultured for 7 days. Cell numbers were counted, and viable cell numbers were plotted. Conditioned medium: a 2 day-culture supernatant from cells expressing inducible ZNF777-wt seeded at 90,000 cells/cm^2 in the presence of Dox. (D) HCT116 cells expressing inducible ZNF777-wt were treated with (+) or without (−) Dox for 1 day. Whole cell lysates were subjected to Western blotting, using anti-ZNF777 and anti-actin antibodies. Full-length blots are presented in Supplementary Fig. S6. (E) HCT116 cells expressing inducible ZNF777-wt were seeded at 500 or 20,000 cells/cm^2, treated with (+) or without (−) Dox after 1 day of culture, and subsequently cultured for 7 days. Viable cell numbers were plotted.

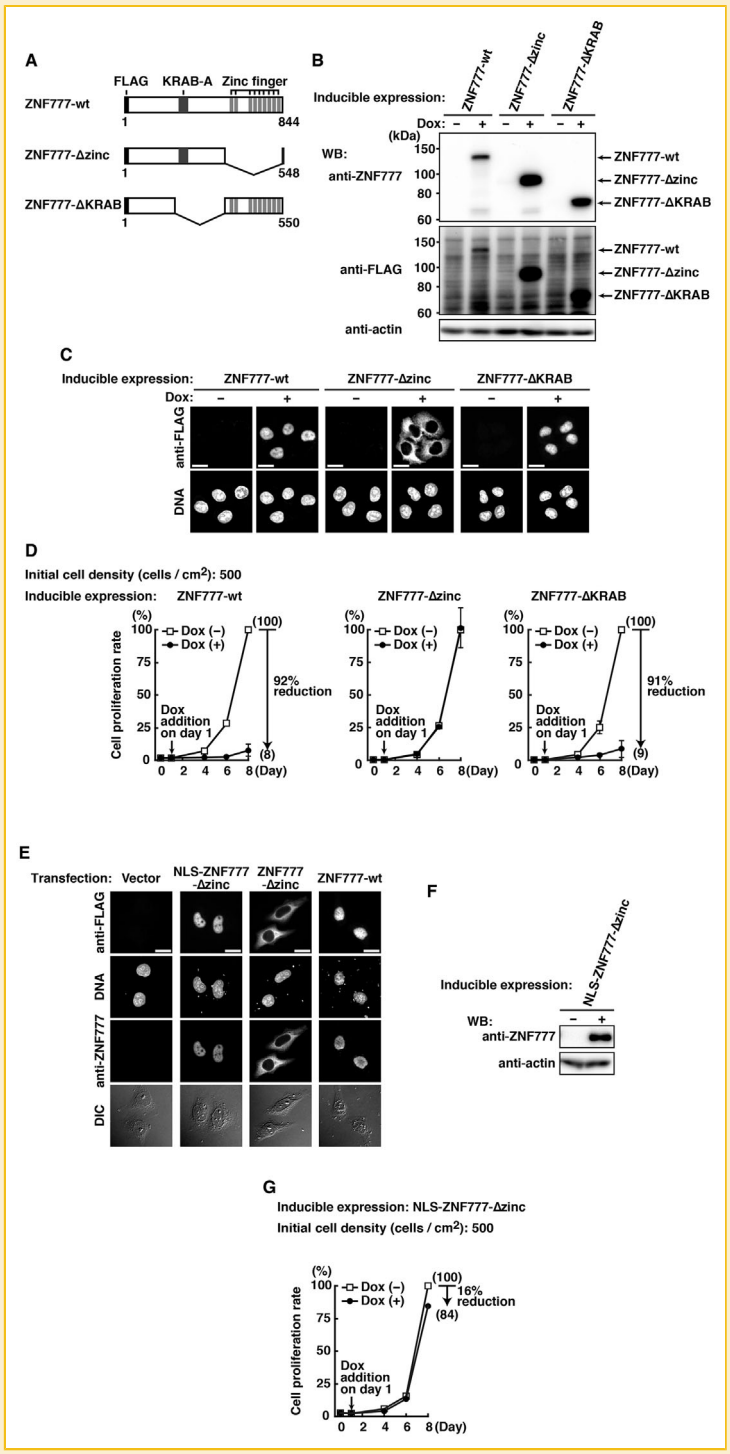

Fig. 5. Role of the zinc finger domain in inhibition of cell proliferation. (A) Schematic representations of ZNF777-wt, ZNF777-Δzinc, and ZNF777-ΔKRAB. (B, C) HeLa S3 cells expressing inducible ZNF777-wt, ZNF777-Δzinc, or ZNF777-ΔKRAB were treated with (+) or without (−) Dox for 1 day. (B) Whole cell lysates were subjected to Western blotting, using anti-FLAG, anti-ZNF777 and anti-actin antibodies. Full-length blots are presented in Supplementary Fig. S7A. (C) Cells were fixed with methanol and doubly stained with anti-FLAG antibody and PI. Scale bars, 20 μm. (D) HeLa S3 cells expressing inducible ZNF777-wt, ZNF777-Δzinc, or ZNF777-ΔKRAB were seeded at 500 cells/cm^2, treated with (+) or without (−) Dox after 1 day of culture, and subsequently cultured for 7 days. Cell numbers were counted, and cell proliferation rates were assessed by measuring the percent ratio of the viable cell number on each day to that on day 8 in the absence of Dox. Bars represent means ± S.D. from three independent experiments. Numbers in parentheses indicate mean values. (E) HeLa cells transfected with vector alone, NLS-ZNF777-Δzinc, ZNF777-Δzinc, or ZNF777-wt were cultured for 24 h. Cells were fixed with methanol and triply stained with anti-FLAG and anti-ZNF777 antibodies and PI. Scale bars, 20 μm. (F) HeLa S3 cells expressing inducible NLS-ZNF777-Δzinc were treated with (+) or without (−) Dox for 1 day. Whole cell lysates were subjected to Western blotting, using anti-ZNF777 and anti-actin antibodies. Full-length blots are presented in Supplementary Fig. S7B. (G) HeLa S3 cells expressing inducible NLS-ZNF777-Δzinc were seeded at 500 cells/cm^2, treated with (+) or without (−) Dox after 1 day of culture, and subsequently cultured for 7 days. Viable cell numbers were plotted.

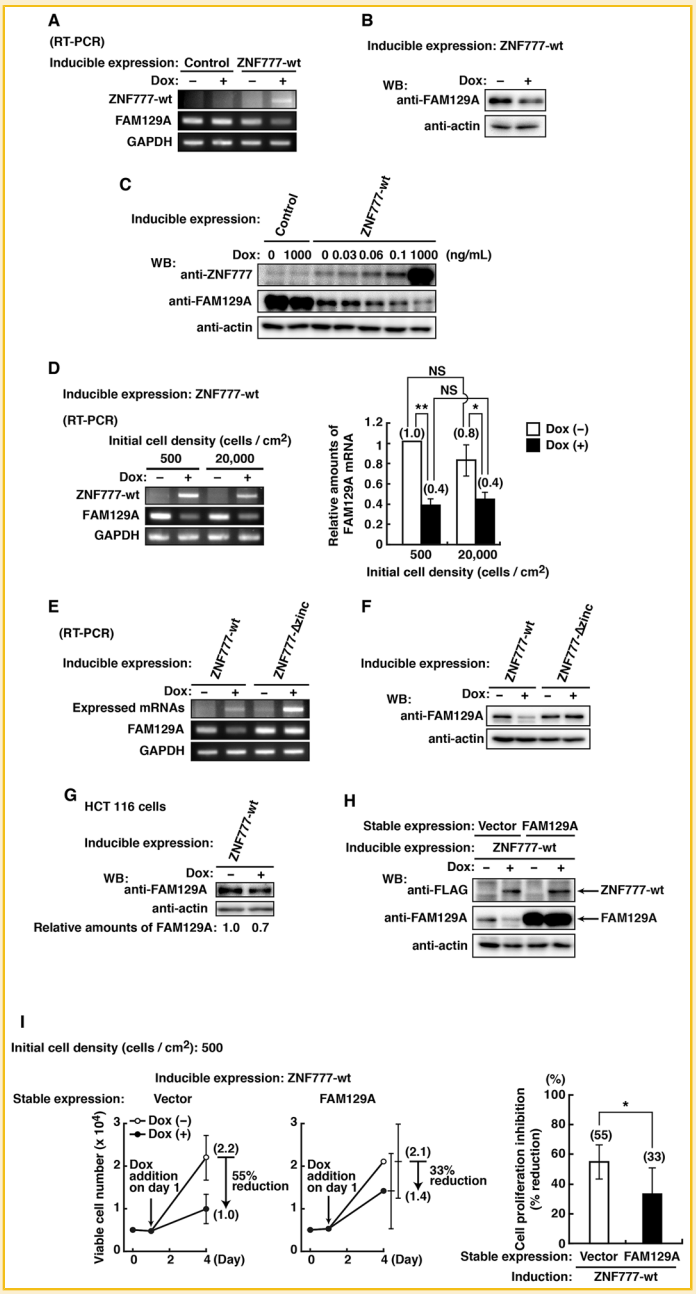

Fig. 6. Involvement of down-regulation of FAM129A in ZNF777-mediated inhibition of cell proliferation. (A, B) Parental HeLa S3/TR cells and HeLa S3 cells expressing inducible ZNF777-wt were treated with (+) or without (−) Dox for 1 day. The levels of FAM129A expression were assessed by semiquantitative RT-PCR (A), and whole cell lysates were subjected to Western blotting, using anti-FAM129A and anti-actin antibodies. Full-length blots are presented in Supplementary Fig. S8A. (C) Parental cells and HeLa S3 cells expressing inducible ZNF777-wt were seeded and treated with Dox at the indicated concentrations for 2 days. Whole cell lysates were subjected to Western blotting, using anti-ZNF777, anti-FAM129A, and anti-actin antibodies. Full-length blots are presented in Supplementary Fig. S8B. (D) HeLa S3 cells expressing inducible ZNF777-wt were seeded at 500 or 20,000 cells/cm^2 and treated with (+) or without (−) Dox for 1 day. The levels of FAM129A expression were assessed by semiquantitative RT-PCR, and the amounts of FAM129A product were quantitated by measuring band intensities and normalizing to the levels of GAPDH. Bars represent means ± S.D. from three independent experiments. Numbers in parentheses indicate mean values, and asterisks indicate the significant difference ($^{*}P < 0.05$; $^{**}P < 0.01$; NS, not significant) calculated by Student's *t*-test. (E, F) HeLa S3 cells expressing inducible ZNF777-wt or ZNF777-Δzinc were treated with (+) or without (−) Dox for 1 day. The levels of FAM129A expression were assessed by semiquantitative RT-PCR (E), and whole cell lysates were subjected to Western blotting, using anti-FAM129A and anti-actin antibodies (F). Full-length blots are presented in Supplementary Fig. S8C. (G) HCT116 cells expressing inducible ZNF777-wt were seeded and treated with Dox for 2 days. Whole cell lysates were subjected to Western blotting, using anti-FAM129A and anti-actin antibodies. Full-length blots are presented in Supplementary Fig. S9A. (H) Following stable expression of FAM129A or vector alone, HeLa S3 cells expressing inducible ZNF777-wt were treated with (+) or without (−) Dox for 1 day. Whole cell lysates were subjected to Western blotting, using anti-FLAG, anti-FAM129A, and anti-actin antibodies. Full-length blots are presented in Supplementary Fig. S9B. (I) Following stably expressing FAM129A or vector alone, HeLa S3 cells expressing inducible ZNF777-wt were seeded at 500 cells/cm^2, treated with (+) or without (−) Dox after 1 day of culture, and subsequently cultured for 3 days. Cell numbers were counted, and viable cell numbers were plotted (left). ZNF777-mediated inhibition of cell proliferation was shown as percent reduction (right), and bars represent means ± S.D. from six independent experiments. Numbers in parentheses indicate mean values, and an asterisk indicates the significant difference ($^{*}P < 0.05$) calculated by Student's *t*-test.

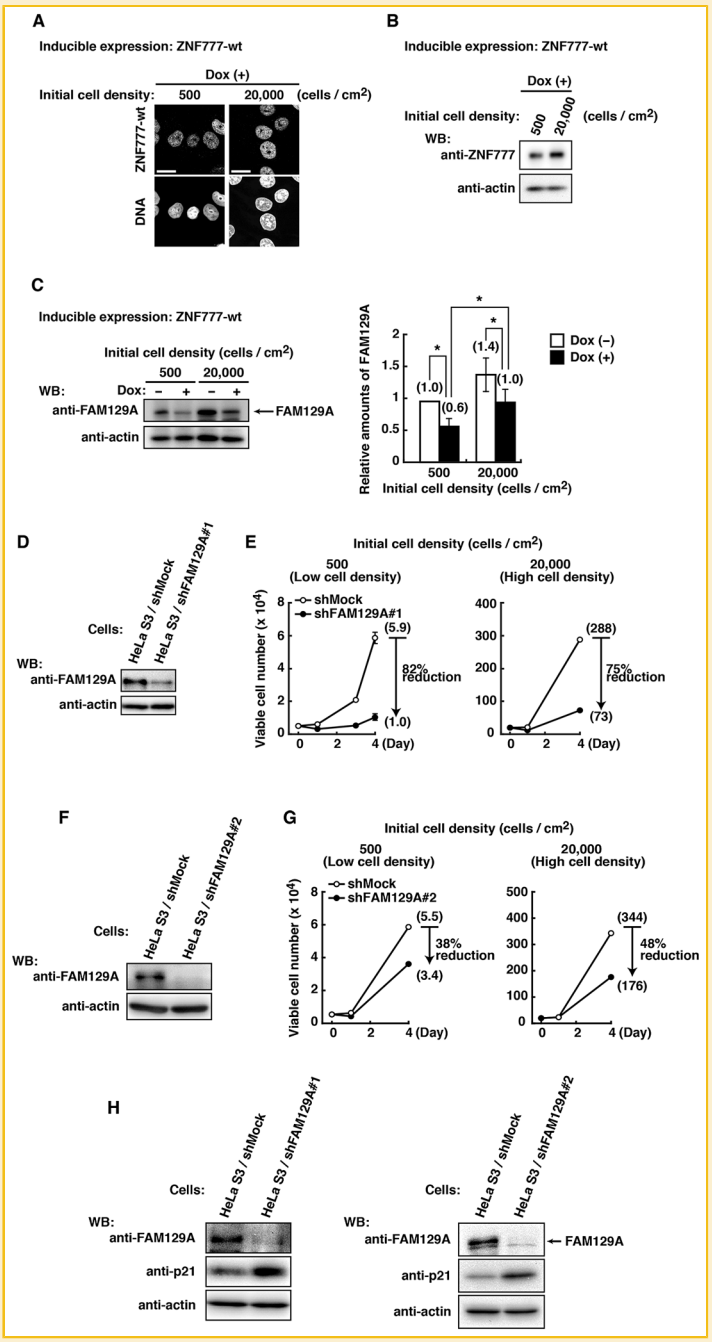

Fig. 7. Cell density-dependent down-regulation of FAM129A. (A, B) HeLa S3 cells expressing inducible ZNF777-wt were seeded at 500 or 20,000 cells/cm^2 and treated with Dox for 1 day. (A) Cells were fixed with methanol and doubly stained with anti-FLAG antibody and PI. Scale bars, 20 μm. (B) Whole cell lysates were subjected to Western blotting, using anti-ZNF777 and anti-actin antibodies. Full-length blots are presented in Supplementary Fig. S10A. (C) HeLa S3 cells expressing inducible ZNF777-wt were seeded at 500 or 20,000 cells/cm^2 and treated with (+) or without (−) Dox for 1 day. Whole cell lysates were subjected to Western blotting, using anti-FAM129A and anti-actin antibodies. Full-length blots are presented in Supplementary Fig. S10B. The amounts of FAM129A were quantitated by measuring band intensities and normalizing to the levels of actin. Bars represent means ± S.D. from three independent experiments. Numbers in parentheses indicate mean values, and an asterisk indicates the significant difference ($^*P < 0.05$) calculated by Student's *t*-test. (D) Whole cell lysates from HeLa S3/Mock-shRNA or HeLa S3/FAM129A-shRNA#1 cells were subjected to Western blotting, using anti-FAM129A and anti-actin antibodies. Full-length blots are presented in Supplementary Fig. S10C. (E) HeLa S3/Mock-shRNA or HeLa S3/FAM129A-shRNA#1 cells seeded at 500 or 20,000 cells/cm^2 were treated with (+) or without (−) Dox after 1 day of culture and subsequently cultured for 3 days. Cell numbers were counted, and viable cell numbers were plotted. Results of cell proliferation initiating at 500 and 20,000 cells/cm^2 were obtained from three and two independent experiments, respectively. Bars represent means ± S.D., and numbers in parentheses indicate mean values. (F) Whole cell lysates from HeLa S3/Mock-shRNA or HeLa S3/FAM129A-shRNA#2 cells were subjected to Western blotting, using anti-FAM129A and anti-actin antibodies. Full-length blots are presented in Supplementary Fig. S11A. (G) HeLa S3/Mock-shRNA or HeLa S3/FAM129A-shRNA#2 cells seeded at 500 or 20,000 cells/cm^2 were treated with (+) or without (−) Dox after 1 day of culture and subsequently cultured for 3 days. Cell numbers were counted, and viable cell numbers were plotted. (H) Whole cell lysates from HeLa S3/Mock-shRNA, HeLa S3/FAM129A-shRNA#1, or HeLa S3/FAM129A-shRNA#2 cells were subjected to Western blotting, using anti-FAM129A, anti-p21, and anti-actin antibodies. Full-length blots are presented in Supplementary Fig. S11B.

protein level of FAM129A, cells expressing inducible ZNF777-wt were seeded at 500 or 20,000 cells/cm^2 and treated with or without Dox for 1 day. ZNF777-wt induction decreased the protein levels of FAM129A both at 500 and 20,000 cells/cm^2 (Fig. 7C). However, at 20,000 cells/cm^2, the decrease in the protein level of FAM129A upon ZNF777-wt induction was insufficient to drastically reduce the rate of cell proliferation (Figs. 4A, 7C). Next, we examined the effect of FAM129 knockdown on cell proliferation. Consistent with the result showing that shRNA against FAM129A strongly decreased the protein level of FAM129A (Fig. 7D, 7F), a strong decrease in the protein level of FAM129A inhibited cell proliferation both at 500 and 20,000 cells/cm^2 (Fig. 7E, 7G). Intriguingly, FAM129A knockdown increased the protein levels of p21 (Fig. 7H), assuming that, unless ZNF777 is overexpressed, FAM129A suppresses the induction of p21. Taken together, these results suggest that a ZNF777-mediated decrease in the protein level of FAM129A at low cell density induces moderate induction of p21, leading to inhibition of cell proliferation.

DISCUSSION

In the present study, we show for the first time that ZNF777 is involved in inhibition of cell proliferation at low cell density. Because overexpression of ZNF777 decreases the expression level of FAM129A, ZNF777-mediated inhibition of cell proliferation is attributable to a decrease in the level of FAM129A. The protein level of FAM129A is strongly decreased at low cell density and moderately decreased at high cell density. A ZNF777-mediated decrease in the level of FAM129A induces moderate levels of p21, leading to a delay in the G2/M phase at low cell density.

ZNF777 is a member of KRAB-ZFPs and is conserved in higher organisms. ZNF777 is ubiquitously expressed, especially in the thymus and liver (see the public RefExA database at http://157.82.78.238/refexa/main_search.jsp). The Oncomine database (http://www.oncomine.com) shows that the expression level of ZNF777 is decreased in some type of cancers, such as follicular lymphoma [Rosenwald et al., 2001]. A decrease in the level of ZNF777 may cause carcinogenesis in such tissues.

The apparent molecular mass of ZNF777 is approximately 35 kDa higher than the predicted molecular mass (Fig. 1B). The retardation of electrophoretic mobility is attributed to the region including the KRAB domain, which corresponds to the amino acids 590–883 of ZNF777 (Fig. 5B). Because the region including the KRAB domain has a large number of negative-charged amino acid residues, it is possible that a reduction in SDS binding to ZNF777 causes the retardation of electrophoretic mobility. Alternatively, it may be also possible that a carbohydrate chain with a molecular mass of approximately 35 kDa is attached to the region including the KRAB domain of ZNF777, because many transcription factors are known to be modified by glycosylation [Vosseller et al., 2002].

It is known that KRAB-ZFPs have a KRAB domain and a zinc finger domain [Gebelein and Urrutia, 2001]. With regard to ZNF777, the zinc-finger domain is responsible for inhibition of cell proliferation, whereas the KRAB domain is not essential for the inhibition of cell proliferation (Fig. 5D, 5G). We further show that ZNF777 localizes to the nucleus in a manner dependent on its zinc-finger domain (Fig. 5C). Since nuclear pore complexes restrain free passage of proteins larger than approximately 40 kDa [Weis, 2003], the translocation of ZNF777 into the nucleus must be an active process involving specific NLSs. In general, a zinc-finger domain has both NLSs and DNA binding motifs [LaCasse and Lefebvre, 1995; Miyamoto et al., 2012]. However, ZNF777 may be accumulated in the nucleus through a putative non-classical NLS in its zinc-finger domain, because ZNF777 has no classical NLS sequence in its primary structure.

A two- to four-fold increase in expression of ZNF777 over endogenous levels was unintentionally leaked in cells expressing inducible ZNF777 without Dox treatment [Fig. 3A, 3D, compare control Dox(−) with ZNF777 Dox(−)]. Considering that the slight increase in expression of ZNF777 by leakiness decreases the number of viable cells on day 8 (Fig. 3C, none Dox(−): $141.5 \pm 30.9 \times 10^4$ cells, ZNF777 Dox(−): $50.1 \pm 4.9 \times 10^4$ cells), only a two- to four-fold increase in expression of ZNF777 is sufficient to inhibit cell proliferation. Moreover, a decrease in the protein level of FAM129A and an increase in the p21 level were observed in cells expressing inducible ZNF777 in a Dox-concentration dependent manner (Fig. 6C, 3I). Overexpression of ZNF777 inhibits cell proliferation possibly owing to a delay in the G2/M phase through moderate expression of p21 (Fig. 3I, 3J). These results suggest that an expression level of ZNF777 positively correlates with an induction level of p21, leading to inhibition of cell proliferation.

FAM129A, also called as Niban, is highly expressed in various types of cancers and is considered to be a candidate marker for some cancer types [Majima et al., 2000; Adachi et al., 2004; Matsumoto et al., 2006; Ito et al., 2010]. The expression level of FAM129A is increased in follicular lymphoma [Rosenwald et al., 2001], suggesting the possibility that a negative correlation between ZNF777 and FAM129A levels is involved in carcinogenesis in some type of tissues. FAM129A is also found to promote cell survival, because FAM129A activates the protein translation machinery undergoing dephosphorylation of eukaryotic translational initiation factor 2α (eIF2α) [Sun et al., 2007]. Conversely, phosphorylation of eIF2α is involved in inhibition of protein translation and induction of p21 [Ye et al., 2010]. In fact, considering that ZNF777 decreases mRNA and protein levels of FAM129A (Fig. 6A, 6B), inhibition of protein translation and induction of p21 may be involved in ZNF777-mediated inhibition of cell proliferation. Upon ZNF777 induction, the number of dead cells is increased from day 6 (Fig. 3C, right panels). Given that FAM129A knockdown increases the number of dead cells by inhibition of protein translation [Sun et al., 2007], it is possible that ZNF777-induced cell death from day 6 is attributed to an inhibition of protein translation. Intriguingly, a strong decrease in the level of FAM129A by shRNA against FAM129A drastically inhibits cell proliferation (Fig. 7D-7G). Because the level of FAM129A is partially decreased upon ZNF777 overexpression (Fig. 6B, 6G, 6H), ZNF777-mediated inhibition of cell proliferation is not completely rescued by FAM129A overexpression (Fig. 6I). We therefore hypothesize that FAM129A and another gene product(s) are involved in ZNF777-mediated inhibition of cell proliferation.

We show that ZNF777 inhibits cell proliferation at low cell density (Fig. 4A, lower panels), suggesting that ZNF777 plays a regulatory role in

cell proliferation depending on cell density. Considering that ZNF777 induces a strong decrease in the mRNA levels of FAM129 at low and high cell densities through the zinc-finger domain (Fig. 6D-6F), we assume that ZNF777 functions as a transcription repressor of FAM129A. Furthermore, ZNF777 induces a strong decrease in the protein level of FAM129 at low cell density, but decreased protein levels of FAM129A at high cell density do not reach those at low cell density (Fig. 7C). A strong decrease in the protein level of FAM129A by knockdown of FAM129A drastically inhibits cell proliferation at both low and high cell densities (Fig. 7D-7G). Taken together, these results suggest that a protein level of FAM129A correlates with a degree of cell proliferation.

Previous studies have been shown that a high cell density condition promotes cell proliferation and survival, which is mediated by soluble growth factors secreted from cells into the culture medium [Sandstrom and Buttke, 1993; Ishizaki et al., 1995; Hearn et al., 1998; Pilling et al., 2000; Ma et al., 2010]. For instance, fibroblast growth factor two increases cell proliferation rates at both low cell density and high cell density [Bianchi et al., 2003]. Interleukin-6 promotes proliferation of a single hybridoma cell and is found in commercially available cloning media [Astaldi et al., 1980; Bazin and Lemieux, 1987; van Oers et al., 1988]. Sphingosine-1-phosphate, a lipid mediator, is shown to inhibit cell proliferation at low cell density and promote cell proliferation at high cell density [Gennero et al., 2002]. In this study, ZNF777 strongly inhibits cell proliferation at low cell density and slightly inhibits cell proliferation at high cell density (Fig. 4A, lower panels). Upon ZNF777 induction at low cell density, cell proliferation can be promoted by addition of conditioned medium in a manner dependent on concentrations of conditioned medium from high-density cultured cells (Fig. 4C). Because cells in general secrete growth factors into the culture medium, a secreted putative growth factor(s) may be involved in ZNF777-mediated inhibition of cell proliferation at high cell density. Considering that, upon ZNF777 induction, protein levels of FAM129A at high cell density are not decreased to those at low cell density (Fig. 7A), we can speculate that a high cell density condition may stabilize FAM129A or inhibit protein degradation of FAM129A. A ZNF777-induced decrease in the protein level of FAM129A at high cell density may be repressed by a secreted putative growth factor(s). Alternatively, it might be also possible that a ZNF777-induced decrease in the protein level of FAM129A at high cell density is repressed by a high degree of cell-cell contact, because a cell density correlate with a degree of cell-cell contact.

In conclusion, we show that ZNF777 inhibits cell proliferation through p21 induction by down-regulation of FAM129A at low cell density, which depends on its zinc finger domain but independent of its KRAB domain. Further studies will help us to better understand the relationship between cell density and cell proliferation.

ACKNOWLEDGMENTS

We are grateful to Ikue Kikuchi, Yusuke Akazawa and Yuji Nakayama for technical help and suggestions. This work was supported in part by grants-in-aid for Scientific Research, Global COE Program (Global Center for Education and Research in Immune Regulation and Treatment) and Special Funds for Education and Research (Development of SPECT probes for Pharmaceutical Innovation) from the Japanese Ministry of Education, Culture, Sports, Science and Technology. K.A., S.K. and H.H. were G-COE Research Assistants, and M.M. is an LGS (Program for Leading Graduate Schools) Research Assistant.

REFERENCES

Adachi H, Majima S, Kon S, Kobayashi T, Kajino K, Mitani H, Hirayama Y, Shiina H, Igawa M, Hino O. 2004. Niban gene is commonly expressed in the renal tumors: A new candidate marker for renal carcinogenesis. Oncogene 23:3495–3500.

Agata Y, Matsuda E, Shimizu A. 1999. Two novel Krüppel-associated box-containing zinc-finger proteins, KRAZ1 and KRAZ2, repress transcription through functional interaction with the corepressor KAP-1 (TIF1beta/KRIP-1). J Biol Chem 274:16412–16422.

Aoyama K, Fukumoto Y, Ishibashi K, Kubota S, Morinaga T, Horiike Y, Yuki R, Takahashi A, Nakayama Y, Yamaguchi N. 2011. Nuclear c-Abl-mediated tyrosine phosphorylation induces chromatin structural changes through histone modifications that include H4K16 hypoacetylation. Exp Cell Res 317:2874–2903.

Aoyama K, Yuki R, Horiike Y, Kubota S, Yamaguchi N, Morii M, Ishibashi K, Nakayama Y, Kuga T, Hashimoto Y, Tomonaga T, Yamaguchi N. 2013. Formation of long and winding nuclear F-actin bundles by nuclear c-Abl tyrosine kinase. Exp Cell Res 319:3251–3268.

Astaldi GC, Janssen MC, Lansdorp P, Willems C, Zeijlemaker WP, Oosterhof F. 1980. Human endothelial culture supernatant (HECS): A growth factor for hybridomas. J Immunol 125:1411–1414.

Bazin R, Lemieux R. 1987. Role of the macrophage-derived hybridoma growth factor in the in vitro and in vivo proliferation of newly formed B cell hybridomas. J Immunol 139:780–787.

Bellefroid EJ, Poncelet DA, Lecocq PJ, Revelant O, Martial JA. 1991. The evolutionarily conserved Krüppel-associated box domain defines a subfamily of eukaryotic multifingered proteins. Proc Natl Acad Sci USA 88:3608–3612.

Bellefroid EJ, Marine JC, Ried T, Lecocq PJ, Riviere M, Amemiya C, Poncelet DA, Coulie PG, de Jong P, Szpirer C, Ward DC, Martial JA. 1993. Clustered organization of homologous KRAB zinc-finger genes with enhanced expression in human T lymphoid cells. EMBO J 12:1363–1374.

Bianchi G, Banfi A, Mastrogiacomo M, Notaro R, Luzzatto L, Cancedda R, Quarto R. 2003. Ex vivo enrichment of mesenchymal cell progenitors by fibroblast growth factor 2. Exp Cell Res 287:98–105.

Chernov AV, Baranovskaya S, Golubkov VS, Wakeman DR, Snyder EY, Williams R, Strongin AY. 2010. Microarray-based transcriptional and epigenetic profiling of matrix metalloproteinases, collagens, and related genes in cancer. J Biol Chem 285:19647–19659.

Friedman JR, Fredericks WJ, Jensen DE, Speicher DW, Huang XP, Neilson EG, Rauscher III. 1996. KAP-1, a novel corepressor for the highly conserved KRAB repression domain. Genes Dev 10:2067–2078.

Fukumoto Y, Obata Y, Ishibashi K, Tamura N, Kikuchi I, Aoyama K, Hattori Y, Tsuda K, Nakayama Y, Yamaguchi N. 2010. Cost-effective gene transfection by DNA compaction at pH 40 using acidified, long shelf-life polyethylenimine. Cytotechnology 62:73–82.

Gebelein B, Fernandez-Zapico M, Imoto M, Urrutia R. 1998. KRAB-independent suppression of neoplastic cell growth by the novel zinc finger transcription factor KS1. J Clin Invest 102:1911–1919.

Gebelein B, Urrutia R. 2001. Sequence-specific transcriptional repression by KS1, a multiple-zinc-finger-Krüppel-associated box protein. Mol Cell Biol 21:928–939.

Gennero I, Fauvel J, Nieto M, Cariven C, Gaits F, Briand-Mésange F, Chap H, Salles JP. 2002. Apoptotic effect of sphingosine 1-phosphate and increased sphingosine 1-phosphate hydrolysis on mesangial cells cultured at low cell density. J Biol Chem 277:12724–12734.

Hearn CJ, Murphy M, Newgreen D. 1998. GDNF and ET-3 differentially modulate the numbers of avian enteric neural crest cells and enteric neurons in vitro. Dev Biol 197:93–105.

Huang C, Jia Y, Yang S, Chen B, Sun H, Shen F, Wang Y. 2007. Characterization of ZNF23, a KRAB-containing protein that is down-regulated in human cancers and inhibits cell cycle progression. Exp Cell Res 313:254–263.

Ishibashi K, Fukumoto Y, Hasegawa H, Abe K, Kubota S, Aoyama K, Kubota S, Nakayama Y, Yamaguchi N. 2013. Nuclear ErbB4 signaling through H3K9me3 is antagonized by EGFR-activated c-Src. J Cell Sci 126:625–637.

Ishizaki Y, Cheng L, Mudge AW, Raff MC. 1995. Programmed cell death by default in embryonic cells, fibroblasts, and cancer cells. Mol Biol Cell 6:1443–1458.

Ito S, Fujii H, Matsumoto T, Abe M, Ikeda K, Hino O. 2010. Frequent expression of Niban in head and neck squamous cell carcinoma and squamous dysplasia. Head Neck 32:96–103.

Kasahara K, Nakayama Y, Sato I, Ikeda K, Hoshino M, Endo T, Yamaguchi N. 2007. Role of Src-family kinases in formation and trafficking of macropinosomes. J Cell Physiol 211:220–232.

Kikuchi I, Nakayama Y, Morinaga T, Fukumoto Y, Yamaguchi N. 2010. A decrease in cyclin B1 levels leads to polyploidization in DNA damage-induced senescence. Cell Biol Int 34:645–653.

Kubota S, Fukumoto Y, Aoyama K, Ishibashi K, Yuki R, Morinaga T, Honda T, Yamaguchi N, Kuga T, Tomonaga T, Yamaguchi N. 2013. Phosphorylation of KRAB-associated protein 1 (KAP1) at Tyr-449, Tyr-458, and Tyr-517 by nuclear tyrosine kinases inhibits the association of KAP1 and heterochromatin protein 1α (HP1α) with heterochromatin. J Biol Chem 288:17871–17883.

Kubota S, Fukumoto Y, Ishibashi K, Soeda S, Kubota S, Yuki R, Nakayama Y, Aoyama K, Yamaguchi N, Yamaguchi N. 2014. Activation of the pre-replication complex is blocked by mimosine through reactive oxygen species-activated Ataxia telangiectasia mutated (ATM) protein without DNA damage. J Biol Chem 289:5730–5746.

Kuga T, Hoshino M, Nakayama Y, Kasahara K, Ikeda K, Obata Y, Takahashi A, Higashiyama Y, Fukumoto Y, Yamaguchi N. 2008. Role of src-family kinases in formation of the cortical actin cap at the dorsal cell surface. Exp Cell Res 314:2040–2054.

LaCasse EC, Lefebvre YA. 1995. Nuclear localization signals overlap DNA-or RNA-binding domains in nucleic acid-binding proteins. Nucleic Acids Res 23:1647–1656.

Looman C, Åbrink M, Mark C, Hellman L. 2002. KRAB zinc finger proteins: an analysis of the molecular mechanisms governing their increase in numbers and complexity during evolution. Mol Biol Evol 19:2118–2130.

Lupo A, Cesaro E, Montano G, Izzo P, Costanzo P. 2011. ZN F224: Structure and role of a multifunctional KRAB-Structure and role of a multifuncZFP protein. Int J Biochem Cell Biol 43:470–473.

Lupo A, Cesaro E, Montano G, Zurlo D, Izzo P, Costanzo P. 2013. KRAB-zinc finger proteins: A repressor family displaying multiple biological functions. Curr Genomics 14:268–278.

Ma Q, Wang Y, Lo AS, Gomes EM, Junghans RP. 2010. Cell density plays a critical role in ex vivo expansion of T cells for adoptive immunotherapy. J Biomed Biotechnol 2010:386545.

Majima S, Kajino K, Fukuda T, Otsuka F, Hino O. 2000. A novel gene "Niban" upregulated in renal carcinogenesis: cloning by the cDNA-amplified fragment length polymorphism approach. Jpn J Cancer Res 91:869–874.

Margolin JF, Friedman JR, Meyer WK, Vissing H, Thiesen HJ, Rauscher III. 1994. Krüppel-associated boxes are potent transcriptional repression domains. Proc Natl AcadSci USA 91:4509–4513.

Matsumoto F, Fujii H, Abe M, Kajino K, Kobayashi T, Matsumoto T, Ikeda K, Hino O. 2006. A novel tumor marker. Niban, is expressed in subsets of thyroid tumors and Hashimoto's thyroiditis. Hum Pathol 37:1592–1600.

Miyamoto Y, Loveland KL, Yoneda Y. 2012. Nuclear importin α and its physiological importance. Commun Integr Biol 5:220–222.

Nakayama Y, Igarashi A, Kikuchi I, Obata Y, Fukumoto Y, Yamaguchi N. 2009. Bleomycin-induced over-replication involves sustained inhibition of mitotic entry through the ATM/ATR pathway. Exp Cell Res 315:2515–2528.

Obata Y, Fukumoto Y, Nakayama Y, Kuga T, Dohmae N, Yamaguchi N. 2010. The Lyn kinase C-lobe mediates Golgi export of Lyn through conformation-dependent ACSL3 association. J Cell Sci 123:2649–2662.

Pilling D, Akbar AN, Shamsadeen N, Scheel-Toellner D, Buckley C, Salmon M. 2000. High cell density provides potent survival signals for resting T-cells. Cell Mol Biol (Noisy-Le-Grand) 46:163–174.

Rosenwald A, Alizadeh AA, Widhopf G, Simon R, Davis RE, Yu X, Yang L, Pickeral OK, Rassenti LZ, Powell J, Botstein D, Byrd JC, Grever MR, Cheson BD, Chiorazzi N, Wilson WH, Kipps TJ, Brown PO, Staudt LM. 2001. Relation of gene expression phenotype to immunoglobulin mutation genotype in B cell chronic lymphocytic leukemia. J Exp Med 194:1639–1648.

Sandstrom PA, Buttke TM. 1993. Autocrine production of extracellular catalase prevents apoptosis of the human CEM T-cell line in serum-free medium. Proc Natl Acad Sci USA 90:4708–4712.

Silva FP, Hamamoto R, Furukawa Y, Nakamura Y. 2006. TIPUH1 encodes a novel KRAB zinc-finger protein highly expressed in human hepatocellular carcinomas. Oncogene 25:5063–5070.

Soeda S, Nakayama Y, Honda T, Aoki A, Tamura N, Abe K, Fukumoto Y, Yamaguchi N. 2013. V-Src causes delocalization of Mklp1, Aurora B, and INCENP from the spindle midzone during cytokinesis failure. Exp Cell Res 1382–1397.

Sun GD, Kobayashi T, Abe M, Tada N, Adachi H, Shiota A, Totsuka Y, Hino O. 2007. The endoplasmic reticulum stress-inducible protein Niban regulates eIF2alpha and S6K1/4E-BP1 phosphorylation. Biochem Biophys Res Commun 360:181–187.

Urrutia R. 2003. KRAB-containing zinc-finger repressor proteins. Genome Biol 4:231.

van Oers MH, van der Heyden AA, Aarden LA. 1988. Interleukin 6 (IL-6) in serum and urine of renal transplant recipients. Clin Exp Immunol 71: 314–319.

Vosseller K, Sakabe K, Wells L, Hart GW. 2002. Diverse regulation of protein function by O-GlcNAc: A nuclear and cytoplasmic carbohydrate post-translational modification. Curr Opin Chem Biol 6:851–857.

Weis K. 2003. Regulating access to the genome: Nucleocytoplasmic transport throughout the cell cycle. Cell 112:441–451.

Witzgall R, O'Leary E, Leaf A, Onaldi D, Bonventre JV. 1994. The Krüppel-associated box-A (KRAB-A) domain of zinc finger proteins mediates transcriptional repression. Proc NatlAcad Sci USA 91:4514–4518.

Ye J, Kumanova M, Hart LS, Sloane K, Zhang H, De Panis DN, Bobrovnikova-Marjon E, Diehl JA, Ron D, Koumenis C. 2010. The GCN2-ATF4 pathway is critical for tumour cell survival and proliferation in response to nutrient deprivation. EMBO J 29:2082–2096.

SUPPORTING INFORMATION

Additional supporting information may be found in the online version of this article at the publisher's web-site.